RSC Advances

This is an *Accepted Manuscript*, which has been through the Royal Society of Chemistry peer review process and has been accepted for publication.

Accepted Manuscripts are published online shortly after acceptance, before technical editing, formatting and proof reading. Using this free service, authors can make their results available to the community, in citable form, before we publish the edited article. This *Accepted Manuscript* will be replaced by the edited, formatted and paginated article as soon as this is available.

You can find more information about *Accepted Manuscripts* in the Information for Authors.

Please note that technical editing may introduce minor changes to the text and/or graphics, which may alter content. The journal's standard Terms & Conditions and the Ethical guidelines still apply. In no event shall the Royal Society of Chemistry be held responsible for any errors or omissions in this *Accepted Manuscript* or any consequences arising from the use of any information it contains.

ROYAL SOCIETY OF CHEMISTRY

www.rsc.org/advances

Conductive Enhancement of Copper/Graphene Composites Based on a High-quality Graphene

Weiping Li [a], Delong Li [a], Qiang Fu [a], Chunxu Pan [a,b*]

[a]*School of Physics and Technology, and Center for Electron Microscopy, Wuhan University, Wuhan 430072, China.*

[b]*Shenzhen Research Institute, Wuhan University, Shenzhen 518057, China.*

*Corresponding Author.

E-mail: cxpan@whu.edu.cn (C. Pan); Tel: +86-27-68752481 ext. 8168

RSC Advances Accepted Manuscript

Abstract:

Copper is a well-known traditional metal and has been widely used for thousands years due to its combination property, especially the electrical conductivity. Any efforts for increasing copper electrical conductivity, even a small percent, will make a great economic effectiveness to the society. In this paper, we report an electrical conductivity enhanced copper/graphene composite based upon the high-quality graphene (HQG) via processes involving graphene-coated copper powders through ball milling, and subsequent spark plasma sintering (SPS).The HQG is converted from regular reduced graphene oxide (RGO)by using a hot-pressing treatment. The experimental results reveal that: 1) Comparing with copper/RGO composite, the electrical conductivity of the copper/HQG composites is increased significantly; 2) The highest electrical conductivity of the copper/HQG composite was obtained at the 1wt. % optimal mass percentage of the HQG, 8% increment was archived when comparing with pure copper. We believe that the electrical conductivity enhancement is related to high electron mobility of the HQG, and formation of a graphene conductive network in the copper/HQG composites. In addition, the hardness of both copper/RGO and copper/HQG composites is much higher than that of pure copper, while the copper/HQG composite shows the highest when the amount of HQG is 0.5wt.%.It is expected that the copper/HQG composites have a broad prospect of applications in electrical and electronics industry, light industry, machinery manufacturing, architecture construction, national defense, etc.

Keyword: Conductivity; Composite; Graphene; High-quality Graphene; Ball milling; Hardness

RSC Advances Accepted Manuscript

1 Introduction

As a new type of two dimensional carbon material, graphene has extremely excellent mechanical, physical and chemical properties, such as high values of specific surface area (2630 m^2/g)[1], high thermal conductivity and electron mobility (thermal conductivity about 5000 $Wm^{-1}K^{-12}$ and the electron mobility up to 2×10^5 $cm^2V^{-1}s^{-1}$at room temperature[3]), excellent mechanical properties, etc. At present, the applications of graphene have drawn extensive attentions throughout the world,[4,5] and it is expected to be widely applied in composites,[6] biology,[7] hydrogen storage,[8] nano-electron devices,[9] transistors,[10] field-emission cathodes,[11] energy storage materials,[12] organic photovoltaics,[13-16] batteries [17] and catalysis in industrial scales.[18] As an area for the first breakthrough and widely applications, the graphene-involved composites, such as polymer/graphene composites and metal/graphene composites, have achieved amulti-functional development, based upon graphene's high excellent strength, great toughness and high electrical conductivity. Especially, the applications of graphene in reinforcing polymer composites for enhancing mechanical property and electrical conductivity have made a great success.[19-21]

However, there are still facing challenges for graphene applications in metal composites, due to reasons including agglomerate tendency in liquids, and poor wettability between graphene and metal, which make difficulties to prepare a high performance metal/graphene composite. Therefore, up to now, there are few works on metal/graphene composites, and the complex preparation methods with low costs.

Electrochemical deposition[22] and laser physical vapordeposition[23] have been proven capable of realizing uniform dispersion of reduced graphene oxide (RGO) in metal matrix for getting metal/graphene composite films. Z. Li et al.[24] successfully prepared the aluminum/RGO composites and found that a composite reinforced with only 0.3 wt.% of RGO showed an 18 and 17% increase in elastic modulus and hardness, respectively. They firstly achieved uniform distribution of RGO in an Al matrix via simple electrostatic interaction between graphene oxide (GO) and Al flakes, and a densified RGO/Al composite was obtained by hot pressing the RGO/Al composite powders.

It is well known that structural integrity and defects-free are two preconditions forgetting excellent properties of graphene. That is to say, there are a close relationship between graphene's property and quality involving species and quantity of defects, and different quality of graphene exhibits enormous variation in its performance. For instance, the graphene prepared by micromechanical cleavage has a high electron mobility up to 2×10^5 $cm^2\cdot V^{-1}\cdot S^{-1}$ [3] and specific surface area (calculated value, ~$2630m^2\cdot g^{-1}$)[1]. However, the RGO

RSC Advances Accepted Manuscript

synthesized by chemical exfoliation with a number of oxygenic functional groups and defects shows a low electron mobility (100 $cm^2 \cdot V^{-1} \cdot S^{-1}$) and smaller specific surface area(700 m^2/g).[25] Therefore, the controllable and large scale preparation of high-quality graphene (HQG) plays a key role for its further applications and guarantees the desired properties.

Recently, chemical exfoliation has been considered as a process with advantages including simple, low cost and mass production.[26,27] But its disadvantages are also fatal, such as poor quality, large amount of defects, and high disorder degree of carbon atoms, which lead to poor properties, and then limits the applications

In our previous work,[28] we developed a simple and effective route to convert RGO to high quality graphene (HQG) by using hot-pressing treatment, at high temperature (1500°C) and moderate pressure (40MPa). The experimental results revealed that the HQG was free of defects and oxygen-containing functional groups on the surface, and had a much higher electron mobility (1000 $cm^2V^{-1}S^{-1}$). Preliminary, we prepared the HQG/poly vinylidene fluoride (PVDF) composite films by spin coating. It was found that the storage modulus of the HQG/PVDF composite was nearly twice higher than that of the RGO/PVDF composite. Comparing with pure PVDF, the storage modulus of the HQG/PVDF composite was eight times higher than that of pure PVDF, and the optimum additive amount of the HQG in PVDF was at between 3 and 5 wt.%.[19]

Copper is a well-known traditional metal and has been widely used for thousands years due to its combination property, especially the electrical conductivity. Any efforts for increasing copper's electrical conductivity, even a small percent, will make a great economic effectiveness to the society. Moreover, SPS is a newly developed rapid sintering technique with a great potential for achieving fast densification results with minimal grain growth in a short sintering time.[29] Because of the SPS reduces impurity segregation at grain boundaries,[30] it can greatly improve the graphene/copper composite during sintering.[31]

In this paper, we present a process for producing a copper/graphene composite. Firstly, preparing the graphene-coated copper powders by ball milling; and then, getting the densified composites via high temperature and high pressure sintering. The electrical performance tests revealed that the electrical conductivity was further enhanced for 8% higher than that of pure copper when 1wt.% high quality graphene (HQG) was added in copper matrix, and it is much better than regular copper/RGO composite. In addition, the mechanical property was also improved. We expect that the present result will open up a new era on copper's industrial applications in the future.

RSC Advances Accepted Manuscript

2 Methods

Preparation of graphite oxide (GO): GO was synthesized from natural graphite(~325mesh, 99.95%) by a modified Hummers method:[32,] 1) The mixture of graphite powders (1.0g), $K_2S_2O_4$ (0.5g) and P_2O_5 (0.5g) was put into an 80 °C solution of concentrated H_2SO_4 (10mL) for 4h. And then, the dark mixture was filtrated by deionized water for several times and dried in a stove; 2) The pre-oxidized graphite was put into 15mL 98% H_2SO_4 and 4g $KMnO_4$ was gradually added when stirring and cooling with ice-water bath; 3) 30mL deionized water was added to the solution after stirred for 2 hours at 35°C; 4) The solution was kept at 85 °C for 30 minutes. And then, 30% H_2O_2 was added to the solution until the color of mixture turn to bright yellow. The GO was obtained after filtration, pickling, washing, and drying. 5) Finally, the GO was kept in a tube furnace (OTF-1200X, HEFEI KE JING, China) under Ar atmosphere at 700 °C (heating rate ~10 °C/min) for 1h to obtain the RGO.[33]

Preparation of the high quality graphene (HQG): The RGO was post-treated at 1500 °C and 40 MPa for 5 min in a Spark Plasma Sintering (SPS) system (SPS-3.20MK-II, Sumitomo Heavy Industries).The HQG was scraped by a knife, and the HQG was obtained after ultrasonication in deionized water for 24hours.

Preparation of the copper/graphene composites: Different contents of RGO or HQG were mixed with copper powders (~5μm, 99.7% produced by Sinopharm Chemical Reagent Co., Ltd), and the mixture was treated by ball milling (QM-3SP4J, Nanjing NanDa Instrument Plant, China) in 1700 r/min for 4 hours by using different diameters balls for the purpose of producing the graphene-coated copper powders. The schematic illustration was shown in Figure 1. Subsequently, the powders were processed at 650 °C and 60 MPa for 5minutes by SPS, and the densified copper composites were prepared.[34]

Characterizations of the samples: The morphologies and microstructures of the graphene sheets and composites were characterized by scanning electron microscopy (SEM, FEI, Netherlands, with the energy spectrum of EDS)operated at 20 kV, high-resolution transmission electron microscope (HRTEM,JEM-2010FEF, JEOL, Japan)operated at200 kV, and Raman spectroscopy (LabRAM HR, HORIBA JobinYvon, France). The power of Raman laser was 15mW, and the laser excitation was 488 nm. Scans were taken on an extended range (1000–3000 cm^{-1}) and the exposure time was 5seconds. Samples were sonicated in ethanol and drop-casted onto a SiO_2 substrate for optical observation. The electrical conductivity of samples was measured by using a precise power source/measure unit (B2902A, Agilent, USA), and the test voltage was continuously changed from -20 mV~20 mV in same distance. And the current-voltage curve was measured at 20 °C. The relative conductivity was calculated from the slope of current-voltage curve.

RSC Advances Accepted Manuscript

3 Results and discussion

In general, Raman spectroscopy is a convenient and effective method for characterizing carbon materials. The G peak (1580cm^{-1}) and 2D peak (2700cm^{-1}) represent the structure and order-degree of carbon materials, and the D peak (1350cm^{-1}) represents the concentration of defects or disorder-degree in graphite. Figure 2 illustrates Raman spectra of samples involving graphite, GO, RGO and HQG, respectively. The 2D peak in graphene is the second order of the D peak and caused by double resonant Raman scattering with two-phonon emissions. The 2D peak is sensitive to the number of graphene layer, in which, the graphene should be free of defect and has no D peak. However, the defects and functional groups will be introduced on the RGO sheets inevitably, which decrease the intensity of 2D peak. Obviously, only G peak and 2D peak remained, and D peak completely disappeared for the HQG, which meant that the oxygenic functional groups and defects on the surface of RGO have been removed after the SPS treatment at high temperature and moderate pressure.

Figure 3 shows SEM morphology of the HQG. Clearly, the graphene still kept in the integrated layers, which indicated that the graphene sheets did not transform into graphite after the hot-pressing treatment. Figure 4 shows HRTEM micrographs of RGO and HQG. It shows the integrated structure and no defect is observed within the HQG directly, which is consistent with Raman spectra. In our previous work,[28] the experimental results revealed that the average electron mobility was about 1000cm^{2}V^{-1}S^{-1} for the HQG sheets (about 8 times higher than the RGO precursor sheets, where the RGO sheets show a mobility of about 130 cm^2 V^{-1} S^{-1}). This high electron mobility of the HQG is of significance to improve the conductivity of the composites.

Figure 5 shows SEM morphologies of the HQG-coated copper powders after ball milling. It can be observed that when the copper powders are coated by graphene sheets, the surface become rough with folds. Actually, the graphene coating structure can be clearly observed from the edge of the copper powders due to the transparency of graphene, as shown in Figure 5(d).

The graphene-coated copper powders were further sintered by SPS to get the densified copper /graphene composite for measuring its electrical conductivity, as shown in Figure 6. The composite bulks are in the size of 10mm diameter and 2 mm thickness after sintering at 650°C and 60MPa for 5 minutes. The gold poles were plated on the composite surface after polished. When measuring the electrical conductivity of the composites, the testing voltage was set continuously from -20 mV to 20 mV, and the current-voltage curves were obtained with a variation of the graphene contents, as shown in Figure 6(b) and Figure 6(c). Comparing to pure copper, the electrical conductivity of the copper/HQG composites changed obviously. That is, when the HQG content was less than 1wt.%, the electrical conductivity increased gradually with increasing the HQG content. However,

RSC Advances Accepted Manuscript

while the content was higher than 1 wt.%, the electrical conductivity began to decrease obviously. And when the HQG content reached to 5 wt.%, the electrical conductivity almost equals to that of pure copper. The highest electrical conductivity of the copper/HQG composite was obtained at the 1wt.% optimal mass percentage of the HQG, 8% increment was archived when comparing with pure copper. However, for the regular copper/RGO composites, the electrical conductivity only increased for 0.3%, as shown in Figure 6(c). Therefore, we believe that the integrated structure and high electron mobility of the HQG play an important role in improving the conductivity of the copper/HQG composites.

In order to explore the mechanism of the variation of electrical properties, we further characterized the microstructures and composition distributions of the copper/HQG composites, as shown in Figure 7 and Figure 8. It was found that with increasing the HQG content, the cavities in the composite gradually increased in quantity and size because of the poor wettability between HQG and copper. That is to say, when a large amount of HQG was added, it will agglomerate and be difficult to be dispersed homogeneously via ball milling. Therefore, during the subsequent SPS treatment, the HQG will become the impurity phases in copper matrix, and formed the cavities. From Figure 8, we can clearly find the carbon distribution within the cavities. That is the reason why the electrical conductivity of the composites was reduced when the HQG contents were overmuch. However, on the other hand, the electrical conductivity could be improved by adding appropriate amount of the HQG.

In fact, according to the Ohm's law, the electrical conductivity of the material can be expressed as:

$$\sigma = ne\mu \tag{1}$$

where n is the carrier concentration in material, e is the electronic charge, and μ is the carrier mobility. According to the quantum statistical theory and periodic boundary conditions, the carrier mobility μ can be expressed as:

$$\mu = \frac{2e}{3m^*}\tau_0(s+3/2)(k_BT)^r \frac{F_{r+1/2}(\xi)}{F_{1/2}(\xi)} \tag{2}$$

where r is the scattering factor, τ_0 is the relaxation time, m^* is the carrier effective mass, s is the spin quantum number, k_B is boltzmann constant, and $F_{1/2}(\xi)$ is Fermi integral function.

According to the formula (2), the main factors affecting the electrical conductivity of materials include scattering factor, effective mass, relaxation time and Fermi level, etc. For a given material system, such as the present copper/graphene composite, all above factors are constant. And thus, regulating microstructures and reducing the scattering of carriers in interface and defects as much as possible are the prominent way to improve carrier mobility.

Figure 9 illustrates the FT-IR spectra of the samples. Obviously, the almost total O-containing

RSC Advances Accepted Manuscript

functional groups had been removed in the copper/HQG composite, which is similar to our previous work.[28] Therefore, we believe that there are two factors related to the enhancement of the conductivity of the copper/HQG composite, i.e., 1) A much higher electron mobility of the HQG than that of regular RGO; 2) An efficient and integrate conductive network of the HQG in the copper matrix. In other words, when the composite has a low HQG content, the contribution to increasing the electrical conductivity is limited because the system cannot construct a whole network structure. However, if the HQG content is overmuch, it is easy to form a large amount of cavities and the scattering of carriers is increased, which makes the electrical conductivity decrease. Therefore, there is an optimum content of the HQG in 1wt.%. As for regular RGO, there is little contribution to increasing the conductivity of copper due to the presence of functional groups and defects in the surface.

In addition, We also measured the hardness of samples by Vickers, as shown in Figure 10. The measurement conditions were 2.942N load force for 20seconds. The hardness of the copper/HQG composite was increased for 13% higher than that of pure copper, when 0.5wt.% HQG was added, and obviously, was higher than that of regular copper/RGO composite.

4 Conclusions

The graphene-coated copper powders were prepared effectively and facilely by using ball milling. Compared to pure copper and regular copper/RGO composite, the copper/HQG composite exhibits an improved electrical conductivity. This is because that the HQG is of an integrated structure without defect due to high temperature and high pressure treatment. It is found that the highest electrical conductivity is archived at the optimal amount 1 wt. % of the HQG, which make 8% increment when compared to pure copper. Based on the present experimental results, the copper/HQG composite is prospective to have great applications in a wide range of areas, such as electrical and electronics industry, machinery manufacturing, architecture construction, national defense, etc.

Acknowledgements

This work was supported by the National Nature Science Foundation of China (Nos. 11174227，51209023),the Special Fund for the Development of Strategic Emerging Industries of Shenzhen City of China (No.JCYJ20140419141154246), and the National Key Technology R&D Program of the Hubei province (No. 2013BHE012).

RSC Advances Accepted Manuscript

Reference

[1] M. D. Stoller, S. Park, Y. Zhu, J. An and R. S. Ruoff, *Nano Letters*, 2008, **8**, 3498-3502.

[2] A. A. Balandin, S. Ghosh, W. Bao, I. Calizo, D. Teweldebrhan, F. Miao, C. N. Lau, *Nano Letters*,2008,**8**, 902-907.

[3] K. I. Bolotin, K. J. Sikes, Z. Jiang, M. Klima, G. Fudenberg, J. Hone, P. Kim, H.L. Stormer, *Solid State Communications*, 2008, **146**, 351-355.

[4] K. S. Novoselov, A. K. Geim, S. V. Morozov, D. Jiang, Y. Zhang, S. V. Dubonos, I. V. Grigorieva, A. A. Firsov, *Science*, 2004, **306**, 666-669.

[5] C. Lee, X. Wei, J. W. Kysar, J. Hone, *Science*, 2008, **321**, 385-388.

[6] S. Stankovich, D. A. Dikin, G. H. B. Dommett, K. M. Kohlhaas, E. J. Zimney, E. A. Stach, R. D. Piner, S. T. Nguyen and R. S. Ruoff, *Nature*, 2006, **442**, 282-286.

[7] C. Chung, Y. Kim, D. Shin, S. Ryoo, B. H. Hong, D. Min, *Acc. Chem. Res.*, 2013, **46,** 2211-2224.

[8] V. Tozzini, V. Pellegrini, *Physical Chemistry Chemical Physics*, 2012, **15,** 80-89.

[9] L. Liao, J. Bai, Y. Lin, Y. Qu, Y. Huang, X. Duan, *Advanced Materials*,2010, **22**, 1941.

[10] K. S. Novoselov, A. K. Geim, S. V. Morozov, D. Jiang, M. I. Katsnelson, I. V. Grigorieva, S. V. Dubonos, A. A. Firsov, *Nature*, 2005, **438,** 197-200.

[11] G. Viskadouros, D. Konios, E. Kymakis, E Stratakis, *Applied Physics Letters*, 2014, **105**, 203104 - 203104-5.

[12] W. Wu, Z. Liu, L. A. Jauregui, Q. Yu, R. Pillai, H. Cao, J. Bao, Y. P. Chen, S. Pei, *Sensors and Actuators B: Chemical*, 2010, **150**, 296-300.

[13] S. Emmanuel, S. Kyriaki, K. Dimitrios, P. Constantinos, K. Emmanuel, *Nanoscale*, 2014, **6**, 6925-6931.

[14] G. Kakavelakis, D. Konios, E. Stratakis, E. Kymakis, *Chemistry of Materials*, 2014, **26**,5988-5993.

[15] D. Konios, C. Petridis, G. Kakavelakis, M. Sygletou, K. Savva, E. Stratakis, E. Kymakis, *Advanced Functional Materials*, 2015, **25**, 2213-2221.

[16] N. Balis, D. Konios, E. Stratakis, E. Kymakis, *Chem. Nano Mat.,* 2015,DOI: 10.1002/cnma.201500044.

[17] J. Hassoun，F. Bonaccorso, M. Agostini, M. Angelucci, M. G. Betti, R. Cingolani, M. Gemmi, C. Mariani, S. Panero, V. Pellegrini, B. Scrosati, *Nano Letters*, 2014, **14**, 4901-4906.

[18] M. Winter, R. J. Brodd, *Chemical Reviews*, 2004, **104**, 4245-4269.

[19] C. Yu, D. Li, W. Wu, C. Luo, Y. Zhang, C. Pan, *Journal of Materials Science*, 2014, **49**, 8311-8316.

[20] S. Ansari, E. P. Giannelis, *Journal of Polymer Science Part B: Polymer Physics*, 2009, **47**, 888-897.

[21] H. Zhang, W. Zheng, Q. Yan, Y. Yang, J. Wang, Z. Lu, G. Ji, Z. Yu, *Polymer*, 2010, **51**, 1191-1196.

[22] G. Xie, M. Forslund, J. Pan, *ACS Applied Materials & Interfaces*, 2014, **6**, 7444-7455.

[23] K. Jagannadham, *Journal of Applied Physics*, 2011, **110**, 074901.

[24] Z. Li, G. Fan, Z. Tan, Q. Guo, D. Xiong, Y. Su, Z. Li, D. Zhang, *Nanotechnology*, 2014, **25**, 325601.

[25] M. J. McAllister, J. Li, D. H. Adamson, H. C. Schniepp, A. A. Abdala, J. Liu, M. Herrera-Alonso, D. L. Milius, R. Car, R. K. Prud'homme, I. A. Aksay, *Chemistry of Materials*, 2007, **19**, 4396-4404.

[26] L. Sun，B. Fugetsu, *Materials Letters*, 2013, **109**, 207–210.

[27] D. Konios, M. M. Stylianakis, E. Stratakis, E. Kymakis, *Journal of Colloid and Interface Science*, 2014, **430**, 108–112.

RSC Advances Accepted Manuscript

[28] Y. Zhang, D. Li, X. Tan, B. Zhang, X. Ruan, H. Liu, C. Pan, L. Liao, T. Zhai, Y. Bando, S. Chen, W. Cai, R. S. Ruoff,*Carbon*,2013, **54**, 143-148.

[29] V. Mamedov, *Powder Metallurgy*, 2002, **45**(4), 322-328.

[30] Z. A. Munir, U. Anselmi-Tamburini , M. Ohyanagi, *Journal of Materials Science*, 2006, **41**(3), 763-777.

[31] L. D. Wang, Y. Cui, S. Yang, B. Li, Y. Liu, P. Dong, J. Bellah, G. Fan, R. Vajtai, W. Fei, *RSC Advances,* 2015, **5,** 19321-19328.

[32] W. S. Hummers, R. E. Offeman, *Journal of the American Chemical Society*,1958, **80**, 1339-1339.

[33] N. I. Kovtyukhova, P. J. Ollivier, B. R. Martin, T. E. Mallouk, S. A. Chizhik, E. V. Buzaneva, A. D. Gorchinskiy, *Chemistry of Materials*, 1999, **11**, 771-778.

[34] Y. Cui, L. Wang, B. Li, G. Cao, W. Fei, *Acta Metallurgica Sinica*, 2014, **27**, 937-943.

RSC Advances Accepted Manuscript

A.

Figure captions:

Figure 1 Schematic illustration of fabrication process for the copper/HQG composite by ball milling.

Figure 2 Raman spectra of graphite, graphite oxide (GO), RGO and HQG.

Figure 3 SEM morphology of the HQG.

Figure 4 HRTEM micrographs of RGO (a) and HQG (b).

Figure 5 SEM morphologies of the HQG-coated copper powders during ball milling. (a) un-coated copper powders; (b) and (c) surfaces of the HQG-coated copper powders; (d) edge of the HQG-coated copper powders.

Figure 6 Electrical conductivity measurements of the composites: (a) densified composites and testing configuration (inset shows the gold electrode on the surface); (b) current-voltage curve of the copper/HQG composites with variant HQG contents (Inset shows the intercept of each line); (c) The relative conductivity relationship of copper/HQG and copper/RGO composites with variant contents.

Figure 7 SEM surface morphologies of the copper/HQG composites with variant HQG contents: (a) 0wt.%; (b) 0.2wt.%; (c) 0.5wt.%; (d) 1wt.%; (e) 3wt.%; (f) 5wt.%.

Figure 8 EDS mapping around the cavity of the copper/HQG composite with 5 wt.% HQG content: (a) SEM morphology; (b) carbon distribution.

Figure 9 FT-IR spectra of pure copper, copper/RGO and copper/HQG

Figure 10 Vickers hardness of the copper/HQG and copper/RGO composites

RSC Advances Accepted Manuscript

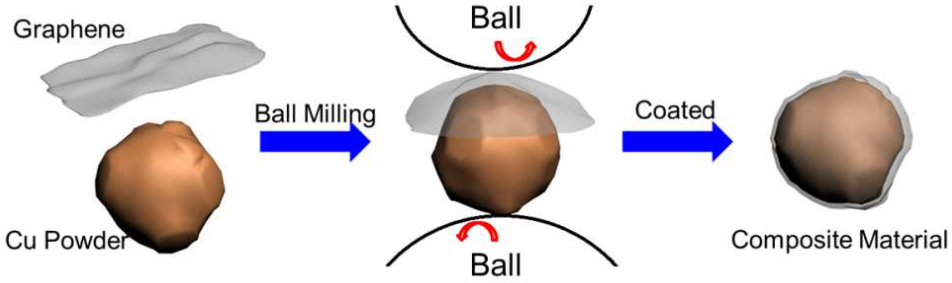

Figure 1 Schematic illustration of fabrication process for the copper/HQG composite by ball milling.

RSC Advances Accepted Manuscript

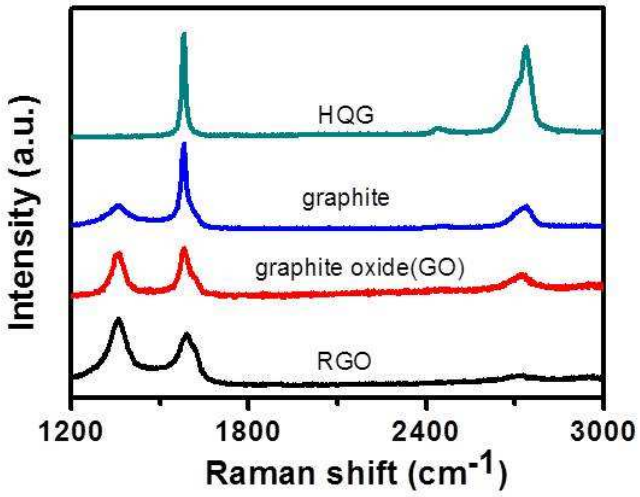

Figure 2 Raman spectra of graphite, graphite oxide (GO), RGO and HQG.

RSC Advances Accepted Manuscript

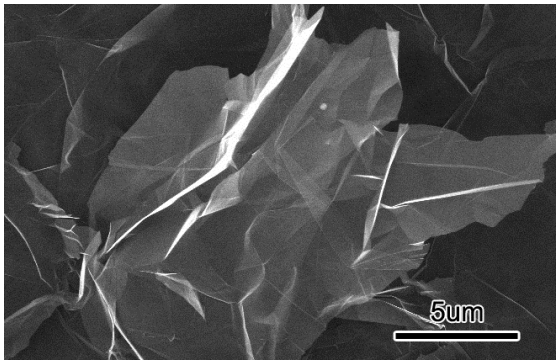

Figure 3 SEM morphology of the HQG.

RSC Advances Accepted Manuscript

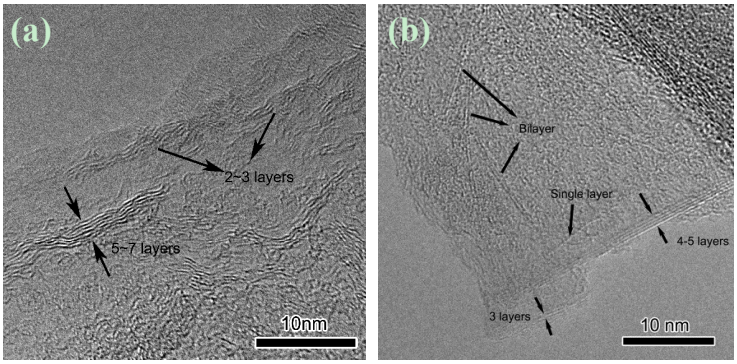

Figure 4 HRTEM micrographs of RGO (a) and HQG (b).

RSC Advances Accepted Manuscript

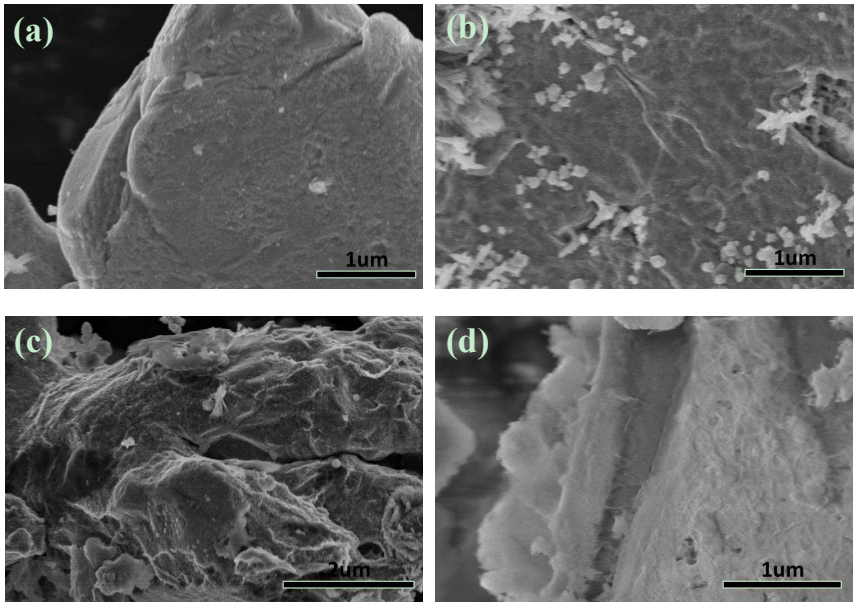

Figure 5 SEM morphologies of the HQG-coated copper powders during ball milling. (a) un-coated copper powders; (b) and (c) surfaces of the HQG-coated copper powders; (d) edge of the HQG-coated copper powders.

RSC Advances Accepted Manuscript

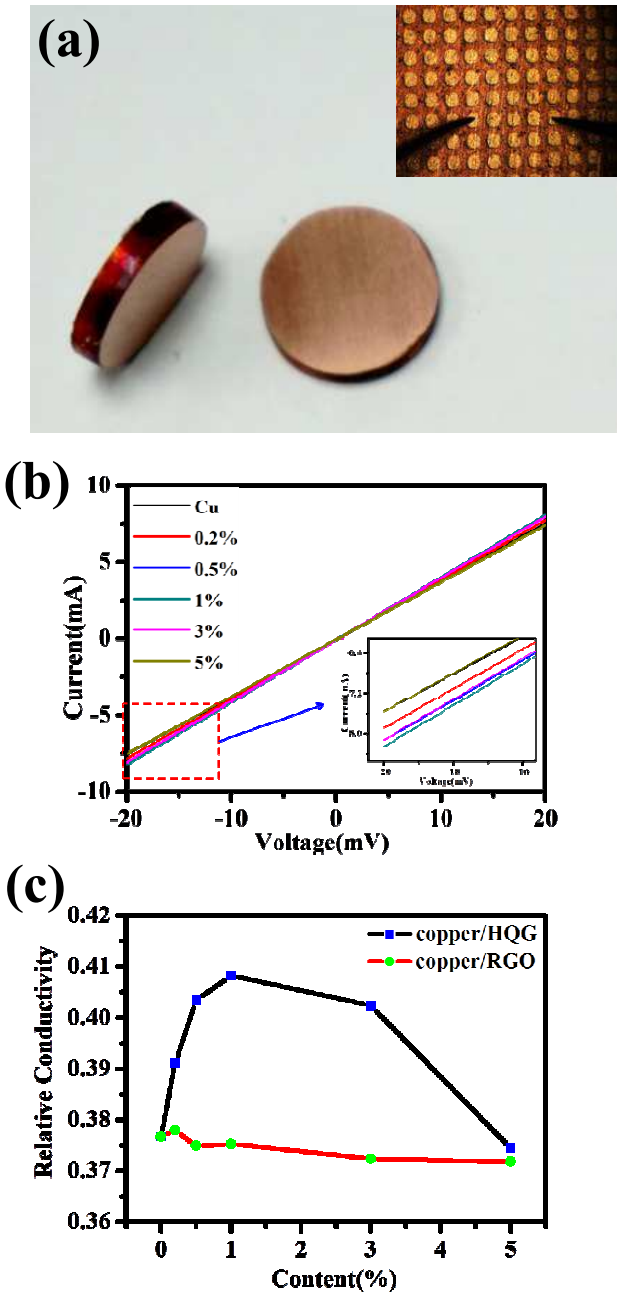

Figure 6 Electrical conductivity measurements of the composites: (a) densified composites and testing configuration (inset shows the gold electrode on the surface); (b) current-voltage curve of the copper/HQG composites with variant HQG contents (Inset shows the intercept of each line); (c) The relative conductivity relationship of copper/HQG and copper/RGO composites with variant contents.

RSC Advances Accepted Manuscript

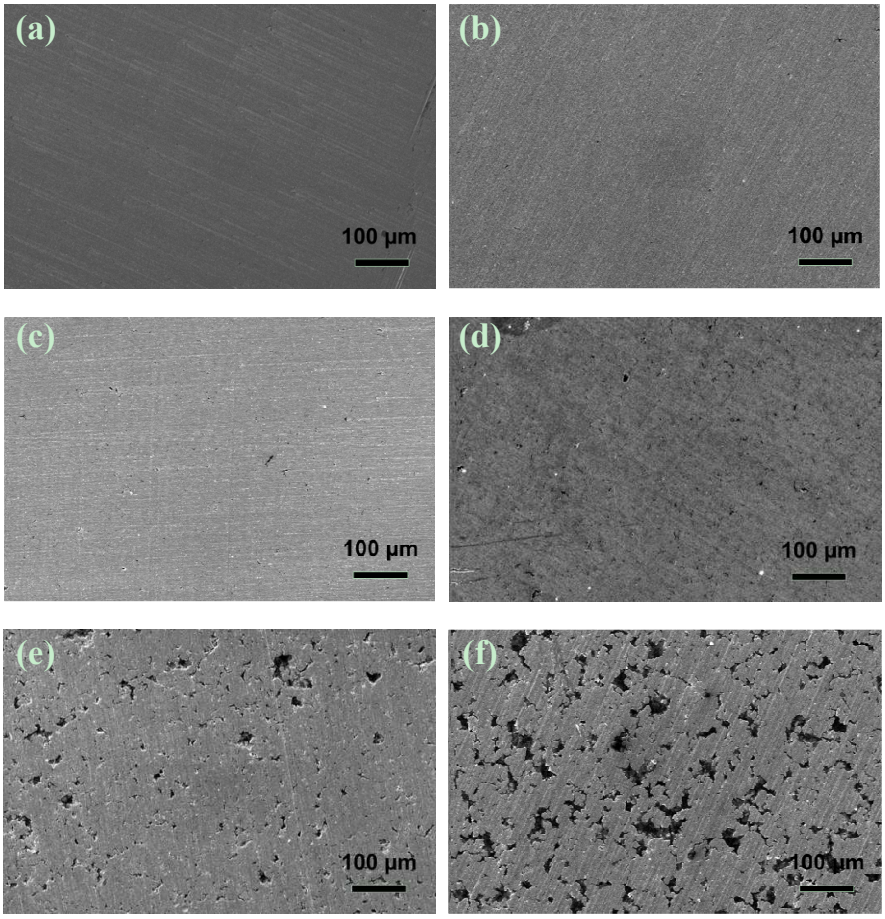

Figure 7 SEM surface morphologies of the copper/HQG composites with variant HQG contents: (a) 0wt.%; (b) 0.2wt.%; (c) 0.5wt.%; (d) 1wt.%; (e) 3wt.%; (f) 5wt.%.

RSC Advances Accepted Manuscript

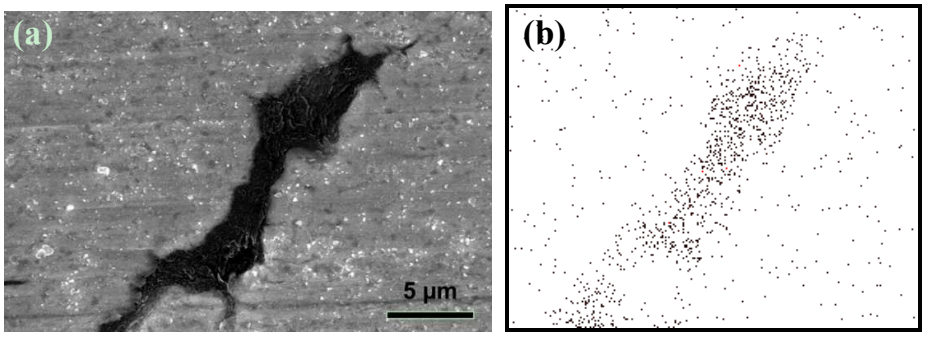

Figure 8 EDS mapping around the cavity of the copper/HQG composite with 5wt.% HQG content: (a) SEM morphology; (b) carbon distribution.

RSC Advances Accepted Manuscript

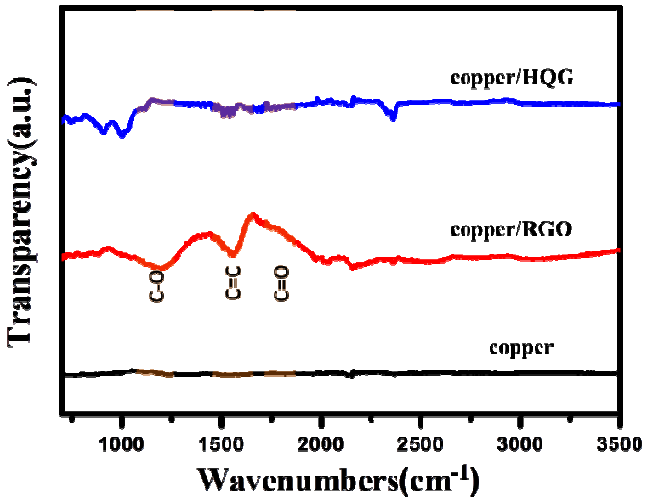

Figure 9 FT-IR spectra of pure copper, copper/RGO and copper/HQG

RSC Advances Accepted Manuscript

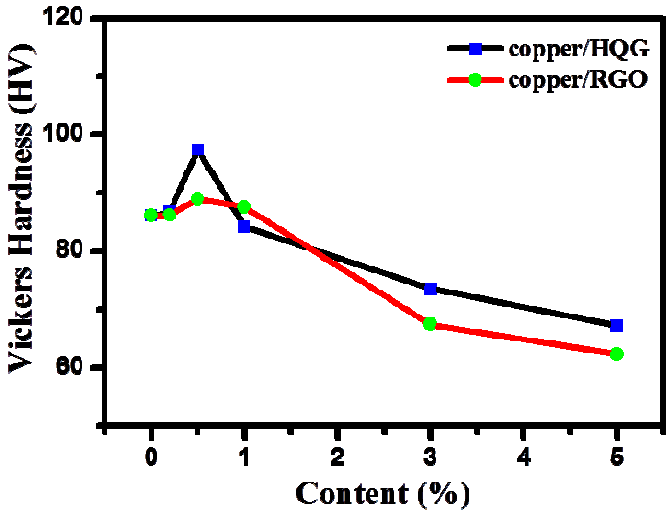

Figure 10 Vickers hardness of the copper/HQG and copper/RGO composites

RSC Advances Accepted Manuscript